

UPCONVERSION AVALANCHE IN THE Yb³⁺/Ho³⁺ DOPED SiO₂-LiYF₄ NANO-GLASS CERAMIC

M. SECU*

Optical Processes in Nanostructured Materials Department

National Institute of Materials Physics, Bucharest-Magurele, 077125, Romania

The “avalanche” up-conversion properties of the glass-ceramics containing (Ho³⁺,Yb³⁺)-doped LiYF₄ nanocrystals have been studied by comparison to the corresponding nanocrystals and polycrystalline powder samples. Under 810 nm laser light pumping, all the samples showed “green” ($^2H_{11/2}, ^4S_{3/2} \rightarrow ^4I_{15/2}$) up-conversion luminescence. The pump power threshold for the avalanche mechanism is about 75mW for the nanocrystalline or polycrystalline powder samples indicating a weak influence of the nanosize related effects is but smaller of about 43mW for the nano-glass ceramic due to the high “local” Yb³⁺ concentrations.

(Received September 12, 2017; Accepted November 6, 2017)

Keywords: nano-glass ceramic, nanocrystals, avalanche up-conversion luminescence,

1. Introduction

New RE³⁺-doped nanoscaled particles embedded in various matrix (i.e. solution, sol-gel-materials, nanoporous etc. [1] and references therein) showing efficient UP-conversion effects (i.e. near-infrared (NIR) conversion into the visible spectral range) [2,3] represent a high potential for applications in various fields (optical amplifiers, optical waveguides, OLEDs, etc.) since they allow the exploitation of the optical phenomena with the optical transparency due to lack of scattering. Such a system is represented by the RE-doped nano-glass ceramic composed by a fluoride nanocrystals embedded in an oxide vitreous matrix. During controlled crystallization of the precursor glass (with appropriate chemical composition and throughout a heat-treatment), one can obtain obtained the partition of the optically active RE³⁺-ions into the precipitated fluoride nanocrystals, with low phonon frequencies, but keeping good chemical and mechanical stability of the oxide glass (see the review of de Pablos-Martin et al. [1]).

One of the most interesting kinds of up-conversion processes is the photon avalanche. The avalanche process is triggered by weak ground state absorption (GSA) to initially populate an intermediate level, from which a resonant excited state absorption (ESA) takes place. Then, an efficient feed-back mechanism, e.g. cross relaxation (CR), connects the emitting level, the intermediate level and the ground level, thus enhancing efficiently. Under certain conditions related to the pumping power, GSA and ESA cross sections and CR rates an efficient enhancement of the population in the intermediate level is reached giving place to the avalanche type process [5,6]. A characteristic feature of the avalanche process is sudden change of the up-conversion intensity dependence on the excitation power at a certain critical pump power. The critical pump indicates the pump power threshold value from which the avalanche mechanism is established [5-8]. For application purposes, it is useful to reduce the pump power threshold, so that the avalanche regime to be reached at relatively low excitation power. Many rare-earth (RE) activated systems have shown photon avalanche processes (see [9] and references within); Ho³⁺-related avalanche up-conversion was firstly reported by Liu et al [10]. In order to make the avalanche mechanism more efficient it was used the Yb³⁺-ion as co-dopant. It is very easily introduced in large concentrations in an appropriate assuring a good homogeneity of the Ho³⁺-Yb³⁺ system. However, a Ho³⁺-Yb³⁺ codoped material, the upconversion mechanism becomes more complex because of

* Corresponding author: msecu@infim.ro

additional energy-transfer and back-transfer channels between these two ions. The avalanche UC luminescence mechanism for $\text{Yb}^{3+}/\text{Ho}^{3+}$ systems has been extensively investigated in many other crystalline host materials [11-13], including oxyfluoride glass ceramics [14,15], theoretically and experimentally [5,6].

Recently RE-doped LiYF_4 nanocrystals have received considerable attention in particular for the up-conversion (UC) properties and related applications, leading to an increased interest for the nanochemistry of this compound. In particular, sol-gel route (using metal alkoxides and involving trifluoroacetic acid as in-situ fluorination reagent [16]) with its advantages: lower processing temperature, the ability to control the purity and homogeneity of the final materials on a molecular level and the large compositional flexibility has been successfully used [17,18].

The aim of the paper is to study and to characterize the avalanche up-luminescence properties (i.e. near-infrared (NIR) conversion into the visible spectral range) of the glass-ceramics containing $(\text{Ho}^{3+}, \text{Yb}^{3+})$ -doped LiYF_4 nanocrystals by comparison to the corresponding nanopowders and polycrystalline ceramic.

2. Experimental

2.1 Samples preparation

For the preparation of the oxyfluoride nano-glass ceramic containing $\text{Yb}^{3+}/\text{Er}^{3+}$ co-doped LiYF_4 nanocrystals we have used the sol-gel route using metal alkoxides and involving trifluoroacetic acid as in-situ fluorination reagent according to the method described in refs. [17,18]. In the first step, tetraethoxysilane (TEOS) was hydrolyzed under constant stirring with a mixed solution of ethanol and water and using glacial acetic acid as catalyst; molar ratio for $\text{TEOS}:\text{EtOH}:\text{H}_2\text{O}:\text{CH}_3\text{COOH}$ was 1:4:10:0.5. Then, another solution of $\text{Er}(\text{CH}_3\text{COO})_3$, $\text{Yb}(\text{CH}_3\text{COO})_3$, $\text{Y}(\text{CH}_3\text{COO})_3$, $\text{Li}(\text{CH}_3\text{COO})$ and CF_3COOH with the molar ratio for $\text{Er}:\text{Yb}:\text{Y}:\text{Li}:\text{F}$ of 1:4:5:20:179 was prepared by and added to the first solution. In the mixed solution the molar ratio $\text{Er}:\text{Yb}:\text{Y}:\text{Li}:\text{Si}$ was 1:3.9:4.9:19.5:42. After an additional vigorous stirring for 1h, the mixed solution was aged at room temperature in a sealed container and then the obtained wet-gel was dried up to 120 °C to form the xerogel. Glass ceramization was achieved after subsequently annealing in air at 530 °C for 45 min.

For the preparation of the $\text{Yb}(4\%)/\text{Ho}(1\%)$ doped LiYF_4 nanocrystalline powders we have used the sol-gel route using metal acetates and trifluoroacetic acid as in-situ fluorination reagent [18]. A powder mixture of $\text{Ho}(\text{CH}_3\text{COO})_3$ (99.9% Alpha Aesar), $\text{Yb}(\text{CH}_3\text{COO})_3$ (99.9% Alpha Aesar), $\text{Y}(\text{CH}_3\text{COO})_3$ (99.99% Alpha Aesar), and $\text{Li}(\text{CH}_3\text{COO})$ (99.998% Alpha Aesar), was dissolved in a solution made of 8 mL isopropanol (99.5% min. Alpha Aesar), 8mL ethanol (99.8% Sigma Aldrich), with addition of 2mL trifluoroacetic acid (99.5+% Alpha Aesar) and 2mL of water. The transparent sol was stirred for 2h and then it was slowly evaporated at room temperature up to dryness. The as-prepared xerogel powder was dried at 60 °C for 24 h and kept in sealed vessels; the crystallization was achieved by calcination in air for 1h at to 530 °C [18].

For the comparison of the up-conversion properties we have prepared a $\text{Yb}(4\%)/\text{Ho}(1\%)$ doped LiYF_4 polycrystalline sample co-doped with Yb^{3+} (4% mol.) and Ho^{3+} (1% mol.) by using conventional solid state route: stoichiometric mixture of LiF , YF_3 , YbF_3 and HoF_3 were thoroughly ground (down to tens on microns size) and dried at 60 °C. Then, the powder was pressed (as pellets) and sintered at 750 °C for 2 h in dry nitrogen atmosphere.

2.2. Samples characterization

The X-ray diffraction (XRD) measurements have been performed on a BRUKER D8 ADVANCE type X-ray diffractometer, in focusing geometry, equipped with copper target X-ray tube and LynxEye one-dimensional detector.

For the transmission electron microscopy (TEM) examinations we have used a probe-corrected JEM ARM 200F microscope. The morphology of the samples was studied by using a Carl Zeiss EVO 50 scanning electron microscope (SEM).

UP-conversion luminescence measurements have been performed at room temperature by using a commercial Jobin Yvon spectrophotometer Fluoromax 4-P and a laser diode module

centred at 810nm with a maximum power of 1.2W focused to a spot size of about 3 mm diameter. For the power dependence of the up-conversion (UC) luminescence intensity we used a set of neutral filters with different optical transmission.

3. Results and discussion

3.1. X-ray diffraction

The XRD pattern of the glass-ceramic has shown the LiYF_4 nanocrystals precipitation in the glass matrix (JCPDS file no. 081-2254) – Figure.1 accompanied by much smaller peaks due to $\text{Y}_2\text{Si}_2\text{O}_7$ phase (JCCD file no. 076-0204). The XRD pattern analysis (space group $C_{4h}^6(I4_1/a)$) has indicated $d \cong 40$ nm nanocrystals size and lattice constants: $a = b = 5.1696$ nm, $c = 10.694$ nm.

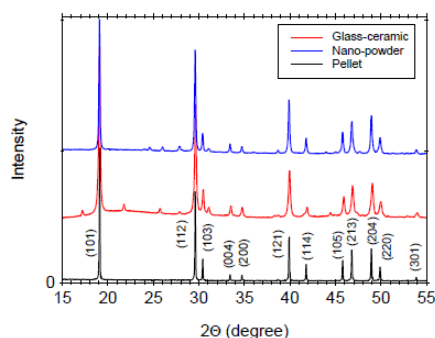


Fig. 1. The XRD patterns of the $\text{Yb}^{3+}/\text{Ho}^{3+}$ co-doped $\text{SiO}_2\text{-LiYF}_4$ nano-glass ceramic (a) and of $\text{LiYF}_4:(\text{Yb}^{3+}/\text{Ho}^{3+})$ nanocrystalline powder compared to the LiYF_4 polycrystalline sample.

The XRD pattern of the $\text{LiYF}_4(\text{Yb},\text{Ho})$ nanocrystalline powders calcinated at 530°C has indicated the formation of the LiYF_4 crystalline phase accompanied by smaller peaks due to the YF_3 phase (JCPDS-file 70-1935). From the XRD pattern analysis (space group $C_{4h}^6(I4_1/a)$) we have extracted the average size of the nanocrystals $d \cong 65$ nm and lattice constants: $a = b = 5.1565$ nm, $c = 10.685$ nm.

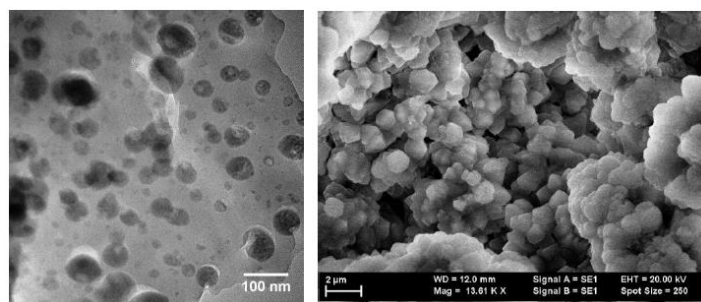


Fig. 2. TEM image of a nano-glass ceramic grain containing LiYF_4 nanocrystals [17] (left); SEM image of the LiYF_4 nanocrystalline powder calcinated at 530°C (right)

3.2. Electron microscopy measurements

The TEM image of a nano-glass ceramic sample grain shows a distribution of nanocrystals of about tens of nm size (Figure.1) [17]. SEM micrographs of the nanocrystalline powders doped with Yb(4%), Ho1(%) calcinated at 530°C showed powder-like microstructures with particle of around hundreds of nm size, much bigger than crystallite size determined by XRD (tens of nm) indicating aggregation and sintering of primary nano-crystallites into microcrystalline particles. It

was shown that LiYF_4 nanocrystals result from an autocatalytic process, where the amorphous sample exhibits a fast self-accelerated crystallization; a second metastable phase (YF_3) acts as the catalyst for the LiYF_4 phase crystallization process. The reaction energy released contributed to the growth, agglomeration and collapsing process of the crystalline fragments, which is consistent with the morphology evidenced by electron microscopy [19].

3.3. Up-conversion luminescence processes

The UC luminescence spectra of $(\text{Ho}^{3+}\text{-Er}^{3+})$ doped $\text{SiO}_2\text{-LiYF}_4$ glass-ceramics and $\text{LiYF}_4:(\text{Yb}^{3+}/\text{Ho}^{3+})$ nanocrystalline or polycrystalline powder under 810nm laser light pumping is presented in Fig. 3; it shows the “green” Ho^{3+} characteristic luminescence assigned to the $(^5\text{S}_2, ^5\text{F}_4) \rightarrow ^5\text{I}_8$ transition [11].

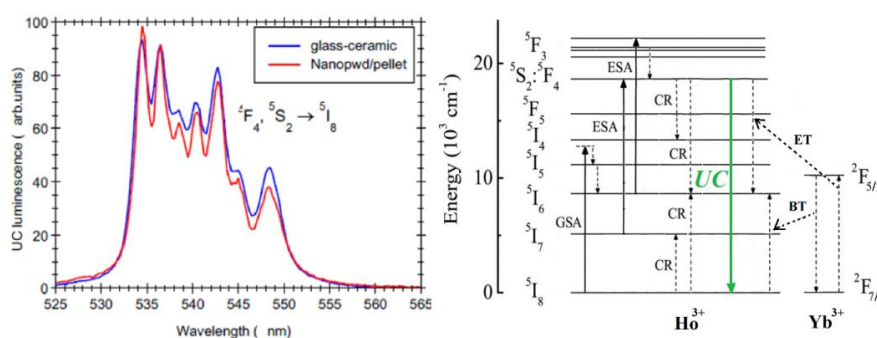


Figure 3. “Up-conversion” luminescence spectra recorded on $(\text{Ho}^{3+}\text{-Er}^{3+})$ doped $\text{SiO}_2\text{-LiYF}_4$ nano-glass ceramic and $\text{LiYF}_4:(\text{Yb}^{3+}/\text{Ho}^{3+})$ nanocrystalline or polycrystalline powder-left; energy levels scheme of Ho^{3+} and Yb^{3+} ions with the main processes leading to the “green” avalanche up-conversion luminescence $(^5\text{F}_4, ^5\text{S}_2) \rightarrow ^5\text{I}_8$ – right.

In order to investigate if a photon avalanche mechanism is responsible for the “green” up-conversion emission of the glass ceramic the avalanche characteristic features are studied. The dependence of the up-conversion emission intensity on the excitation pump power is expected to show a sudden increase close to the pump power threshold [20,21]. Therefore, we have recorded the pump power dependence of the “green emission” $(^5\text{F}_4, ^5\text{S}_2) \rightarrow ^5\text{I}_8$ under 810 nm laser light pumping and we compare it to the nanopowders and polycrystalline sample (pellet) the results being presented in the Figure 4. It can be observed that all the dependencies showed a threshold to the “saturation” regime, typical for the up-conversion avalanche mechanism. Moreover, this threshold is higher for the nanocrystalline or polycrystalline powder sample (pellet) (of about 75mW) compared to the nano-glass ceramic (of about 43mW).

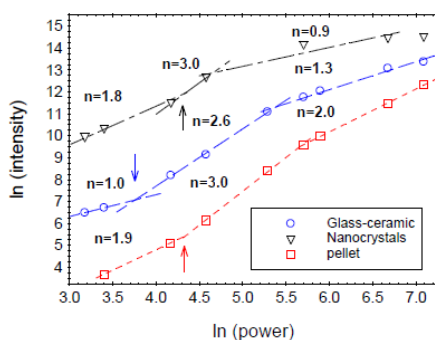


Fig. 4. Pump power dependence in log-log scale of the $(^5\text{F}_4, ^5\text{S}_2) \rightarrow ^5\text{I}_8$ “green emission” recorded under 810 nm laser light pumping on $\text{Yb}^{3+}/\text{Ho}^{3+}$ co-doped $\text{SiO}_2\text{-LiYF}_4$ nano-glass ceramic and $\text{LiYF}_4:(\text{Yb}^{3+}/\text{Ho}^{3+})$ nanocrystalline and polycrystalline powder samples; n represents the slope of the lines.

The avalanche UC luminescence is the result of complex energy transfer (ET), cross-relaxations (CR) and back-transfer (BT) processes, which are strongly dependent on the Yb and Ho concentrations [5,6], and are represented in the energy level scheme in Fig.3. It was supposed that the avalanche process starts with the ground state absorption (GSA) ($^5I_8 \rightarrow ^5I_4, ^5I_5$) followed by non-radiative deexcitation to the 5I_6 and 5I_7 levels, from which the excited state absorption (ESA): $^5I_6 \rightarrow ^5G_6: ^5F_1$ and $^5I_6 \rightarrow ^5G_6: ^5F_1$ take place, with the phonon relaxation to the $^5S_2: ^5F_4$ level. Then, cross relaxation (CR) ($^5S_2: ^5F_4, ^5I_8 \rightarrow (^5I_6, ^5I_6)$), energy transfer (ET) ($^5S_2: ^5F_4, ^2F_{7/2} \rightarrow (^5I_6, ^2F_{5/2})$) and back transfer processes (BT) ($^2F_{5/2}, ^5I_8 \rightarrow (^2F_{7/2}, ^5I_6)$) between Ho^{3+} and Yb^{3+} ions populate the 5I_6 and 5I_6 intermediate levels (Figure 3). Thus avalanche process of the intermediate levels starts giving rise to large population at the emitting ($^5S_2: ^5F_4$) thermalized levels from which an intense green emission (UC) is obtained. In the particular case of the LiYF_4 it has been found that the influence of the ESA from the 5I_6 level is negligible [5].

The theoretical approach of the photon avalanche regime has interpreted the pump power threshold in terms of gain and loss of the population of the intermediate level [5,6]. The model predicts a reduction of the avalanche pump power threshold when the Yb^{3+} concentration increases. The rates of the ET and BT process (both depend on the Yb^{3+} concentration) increases too, leading to an gain of the population of the 5I_7 intermediate level through the $^5I_6 \rightarrow ^5S_2: ^5F_4 \rightarrow ^2F_{5/2} \rightarrow ^5I_7$ looping mechanism (see Fig. 3). In the present case we suppose that the “local” Yb^{3+} concentration is higher in the nanocrystals (in the glass-ceramic) compared to the nanocrystals (powders) and polycrystalline sample (pellet) [20]. Supposing that almost all Yb^{3+} and Ho^{3+} ions are embedded in the nanocrystals their actual concentration might reach 10% (molar) and 3% (molar), respectively. As this threshold is about the same for the nanocrystalline or polycrystalline powder sample this indicates a weak influence of the nanosize related effects.

4. Conclusions

The “avalanche” up-conversion properties of the glass-ceramics containing ($\text{Ho}^{3+}, \text{Yb}^{3+}$)-doped LiYF_4 nanocrystals have been studied by comparison to the corresponding nanocrystals and polycrystalline powder. Under 810 nm laser light pumping, all the samples showed “green” ($^2H_{11/2}, ^4S_{3/2} \rightarrow ^4I_{15/2}$) up-conversion luminescence. The \ln - \ln power dependencies of the up-conversion luminescence showed a sudden change of at a certain critical pump power and a threshold to the “saturation” regime consistent with an avalanche upconversion mechanism. The pump power threshold is about the same for the nanocrystalline or polycrystalline powder sample (pellet) (of about 75mW) indicating a weak influence of the nanosize related effects. However it is reduced to about 43mW because the “local” Yb^{3+} concentration is higher in the nanocrystals (in the nano-glass ceramic) compared to the nanocrystals (powders) and polycrystalline sample.

Acknowledgements

The authors gratefully acknowledge the Romanian Research Ministry (“Core Program 2016-2017”) for the financial support. The authors acknowledge Dr. Elena Matei and Dr. R. Negrea for helping with the electron microscopy analysis.

References

- [1] K. Binnemans, Chem. Rev. **109**, 4283 (2009).
- [2] H. Schäfer, M. Haase, Angew Chem Int Ed Engl. **50**(26) 5808 (2011).
- [3] F. Auzel, Chem. Rev. **104**(1), 139 (2004).
- [4] A. de Pablos-Martin, A. Duran, M. J. Pascual, Int. Mater. Rev. **57**, 165 (2012).
- [5] E. Osiac, I. Sokolska, and S. Kuck, Phys. Rev. B **65**, 235119 (2002).
- [6] F. Lahoz, I. R. Martín, D. Alonso Phys. Rev. **71**, 045115 (2005).

- [7] S. Guy, M. F. Joubert, and B. Jaquier, *Phys. Rev. B* **55**, 8240 (1997).
- [8] R. Martín, C. Goutadier, S. Guy, Y. Guyot, G. Boulon, M.-T. Cohen-Adad, M. F. Joubert, *Phys. Rev. B* **60**, 7252 (1999).
- [9] M. F. Joubert, *Opt. Mater.* **11**, 181 (1999)
- [10] G. K. Liu, Y. H. Chen, and J. V. Beitz, *J. Lumin.* **81**, 7 (1999).
- [11] E. Osiac, S. Kück, I. Sokólska, M. Osiac, *G. Huber Rom Rep Phys*, **60**(4), 937 (2008).
- [12]. Kück and I. Sokólska, *Chem. Phys. Lett.* **325**, 257 (2000).
- [13] F. Lahoz, I. R. Martín, V. L. Guadalupe, J. Méndez-Ramos, V. D. Rodríguez, U. R. Rodríguez-Mendoza, *Opt. Mater.* **25**, 209 (2004).
- [14] P. Babu, I.R. Martín, K. Venkata Krishnaiah, Hyo Jin Seo, V. Venkatramu, C.K. Jayasankar, V. Lavín, *Chemical Physics Letters* **600**, 34 (2014).
- [15] F. Lahoz, I. R. Martín, J. M. Calvilla-Quintero, *Appl. Phys. Lett* **86**, 051106 (2005)
- [16] S. Fujihara, C. Mochizuki and T. Kimura, *J. Non-Cryst. Solids* **244** (1999), 267 (2005).
- [17] C.E. Secu, R.F. Negrea, M. Secu, *Opt. Mater.* **35**, 2456 (2013).
- [18] Go Kawamura, Ryota Yoshimura, Kazunari Ota, Song-Yul Oh, Norio Hakiri, Hiroyuki Muto, Tomokatsu Hayakawa, Atsunori Matsuda, *J. Am. Ceram. Soc.* **96**(2), 476 (2013).
- [19] C. Bartha, C.E. Secu, M. Secu *Ceramics International* **42**, 18732 (2016).
- [20] M. Secu, C.E. Secu, *J. Non-Cryst. Solids* **426**, 78 (2015).